Digital Vector Image Processing of Lid-Driven Rotating Cavity Flow

You-Gon Kim*

(*Received July 23, 1994*)

A flow visualization method entitled Digital Vector Velocimetry (DVV) method is introduced to extract the flow field quantitatively from particle images. This methodis applied to a lid-driven rotating cavity flow. In the DVV method, a time sequence of images are captured by a CCD (Charge Coupled Device) video camera with each frame containing a single-exposure image. All possible velocity vectors between two temporally successive images in the interrogating window are digitally constructed on the digital vectorgram. The most probable velocity vector is identified as the velocity vector of the maximum intensity in the digital vectorgram. The DVV system provides measurement with subpixel accuracy. The dynamic range of the velocity is expanded using feedback analysis that selects consistent velocity vectors.

Key Words : Quantitative Flow Visualization, Rotating Flow, Digital Vector Velocimetry Method, Particle Image Processing

1. Introduction

Flow visualization has been an important tool in observing the fundamental characteristics of a flow field. Flow visualization helps us comprehend the structure of flow motion directly and instantaneously at multiple points. Conventional flow visualization methods, such as dye tracers, hydrogen bubble, and smoke, are limited to qualitative analysis. Review of qualitative flow visualization methods can be found in several literatures (Merzkirch, 1987, and Yang, 1988). In order to obtain quantitative data, measurements using laser Doppler velocimetry (LDV) and hot-wire anemometry can be made at single points. For the steady flow these measurements can be taken repeatedly at different locations to construct the whole velocity field. However, the point-by-point measurement to obtain the data for the whole velocity field is very tedious and time-consuming. If the flow is unsteady, such an attempt becomes very difficult or almost impossible. However, with the recent advance in computer and imaging technology, it has become possible to utilize various techniques with digital processing algorithms to obtain quantitative flow information. An overall view of quantitative flow visualization methods is available in several literatures (Hesselink, 1988, Adrian, 1991 and Chen et al., 1993).

In the present study a quantitative flow visualization method entitled Digital Vector Velocimetry (DVV) method (Kim, 1991) is introduced and applied to a lid-driven rotating cavity flow. In order to measure the velocity from particle images by the DVV method, a time sequence of images are first captured by a CCD (Charge Coupled Device) video camera with each frame containing a single-exposure image. Given a small interrogating window, many velocity vectors may be drawn between two temporally successive images by linking any two particles from the initial image to the following image. These digital velocity vectors may be constructed on a diagram where all the initial particle images are moved to the origin of the diagram. This diagram is called the digital vectorgram. Then the most probable velocity vector can be determined by identifying the position of the maximum veloc-

* Department of Mechanical Engineering Chonnam National University, Kwangju, Korea

ity intensity in the digital vectorgram. Unlike most of the quantitative methods that need optical postprocessing or complicated statistical method to analyze the image taken, the DVV method invokes the direct count of the most probable digital vector. It can be implemented without much computation effort and additional optical system.

In this study the DVV method is employed to measure the velocity field in rotating flows. The selection of rotating flows for the study is because they have important fluid mechanical applications in turbines, turbomachinaries, hydraulic pumps, cyclones, bearings, and swirling in separators. Rotating flows in these devices are in general three-dimensional and highly rotational. The rotating flow fields are difficult to measure due to curved geometry normally associated with the rotating flow. In this investigation the lid-driven rotating cavity flow in the laminar region with Reynolds number of 3200 is quatitatively visualized by the digital vector velocimetry method. The experimental data obtained from the DVV method are quantitatively compared with the numerical results simulated by the finite analytic (FA) method. The comparison reveals good agreement except in the region where the velocity gradient is large within the interrogating element.

2. Experimental System

The major components include (1) test section, (2) light source and optics, (3) light-scattering particles in a test fluid, (4) recording medium, and (5) image processing system. A typical experimental setup is shown in Fig. 1.

2.1 Test section

The basic geometry selected for the present study is a cylindrical cavity with the top lid driven to rotate at a steady angular rotation of 10 rpm. Detailed drawing for the test cell for the lid-driven rotating cavity flow is given in Fig. 2. Plexiglas pipe with 127 mm inside diameter and 12.7 mm thickness is used as the cylindrical wall of the test section. In order to minimize leak between the lid and the cylinder wall, a lid with

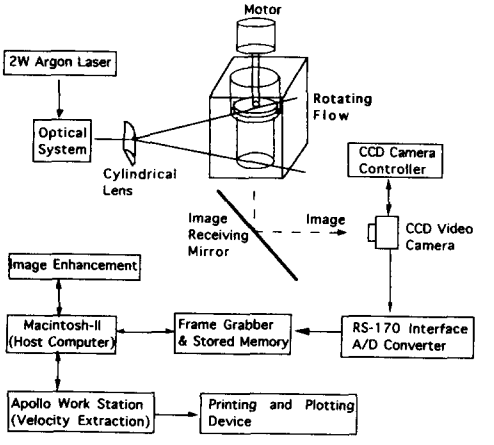

Fig. 1 Overall image processing system

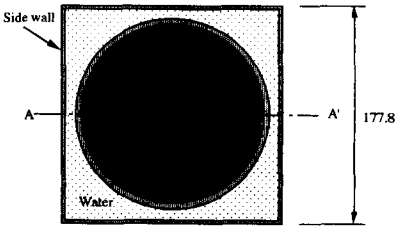

(a) Top view of the test cell

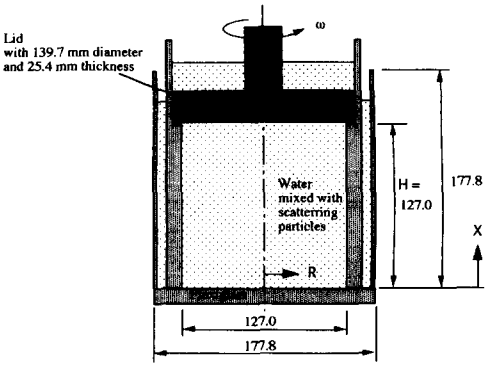

(b) Side view of crosssection A-A'

Fig. 2 Detailed drawing of test cell for lid-driven rotating cavity flow

25.4 mm thickness is used and the gap between the lid and the top of cylinder wall is kept as small as practically possible. In the present study we set the gap as less than 1 mm. The lid-driven disk was constructed such that the gap between the lid and the side of the upper wall is given as 1 mm so that disturbance due to the gap and the

potential leak is minimal and negligible. Water is filled up to at least 15 mm above the lid to avoid generating cavity just beneath the center of the lid due to subatmospheric pressure created by the centrifugal force from the rotating of the fluid. In order to avoid the noise due to the reflection of light from the laser, the lid surface was coated with a black enamel paint.

2.2 Light source and optics

Figure 1 shows the light source and optical arrangement for the experiment. Inova 70 series 2W Argon laser system is used as a light source. This light operates at a wavelength of 514.5 nm. The diameter of the initial beam is 2.5 mm and the beam divergence is given as 0.5 mrad. In the present study of rotating flow the swirl velocity is the primary motion of the flow. Therefore, the swirling motion is greater than the radial or axial motion by an order of magnitude. Thus, if the flow is illuminated from the side by placing a light sheet through the cylinder wall, a light sheet thicker than 2.5 mm is needed to capture the radial and axial motion in the test section. For example, when a swirling velocity at the edge of the lid is 63.5 mm/s, the maximum axial velocity at the middle height ($X=0.5H$) is measured to be about 2.5 mm/s. Therefore, if a thin light sheet is used for taking the image of the side view, the information on the flow field may be lost. From this reason, the beam diameter is deliberately enlarged to about 10 mm. To obtain a 10 mm-thick light sheet, the laser light may travel about 15 m-distance before it arrives at the test section.

The light sheet distributes the available radiant power within the measuring region. Typically the width of the sheet is 100 to 150 mm. The simplest way of producing a two-dimensional light sheet is to use a single rectangular cylindrical lens. For the bottom view of the rotating flow, a 45° inclined mirror may be placed under the test cell. Using the mirror, the image without any distortion, just upside-down, is easily obtained.

2.3 Recording medium

A CCD video camera is used to capture the digital flow images. The CCD video camera used in this study is a NEC model TI-24A. The minimum sensitivity of the CCD is 2 lux, at f-number of 1.4, which is corresponding to 5.8 nW/m^2 with a wavelength $\lambda=514.5$ nm according to CIE (International Commission on Illumination) luminous efficiency curve. The available f-numbers ranges from 1.4 to 20. The pixel resolution is $540(H)\times480(V)$with each pixel area measuring 23 μm 23 μm and the time between frames is 1/30 s (30 Hz). The gray scale of each pixel is given as 8 bit or 256 gray levels from 0 to 255. The shutter speed is set as 1/250 s.

2.4 Scattering particles

To obtain the quantitative measurement of velocity field in a flow, light scattering particles are required to be seeded in the flow. There are three primary requirements for the selection of the tracer particles. First, they must be nearly equal in density to that of the working fluid for neutral buoyancy. Second, the particles must not themselves disturb the flow field, and third, the particles must be detectable by the recording medium. For quantitative flow visualization the lower limit on a particle size is that the light scattered from the particle must be detectable. According to Walter and Chen (1989), the minimum exposure is given as 6.88×10^{-4} mJ/m^2 for the CCD. Based on this value, it is estimated that the CCD can image particles as small as 1 m with a 10 mW He-Ne laser as the light source.

In general, for a successful measurement in the particle image velocimetry (PIV) method (Adrian, 1984, and Landreth et al, 1988), the upper limit for seeding concentration is set by a value above which a speckle pattern is formed. In the digital vector velocimetry (DVV) method, the seeding concentration is limited to that it does not obstruct the light and does not change the fluid properties such as viscosity.

The seeding particle chosen for the experiment in water is Pliolite VT, which is manufactured Goodyear Tire and Rubber Co. of Akron, Ohio. Pliolite VT is vinyltoluene-butadiene copolymer. The mean diameter of the particle is $50\sim100$ μm. The particles are insoluble in water and have an index of refraction of about $n=1.6$. With a spe-

cific gravity of 1.03, they may be considered neutrally buoyant.

2.5 Digital data processing system

Images obtained by the CCD video camera are fed into a microcomputer through a frame grabber interface board, Video Image 1000 board, manufactured by Image System Technology. During the process, the analog signals are converted into digital ones representing the flow field image. The data contained in the time-sequential flow images include displacement information of the particles and time interval between the flow images. Image acquisition and monitoring are accomplished by an image software, called Enhance^{tm}, installed in the Macintosh II computer. In order to obtain a good flow image, one needs to adjust f-number, shutter speed and the laser power. By looking at the real time flow images on the screen of Mac II, one may adjust the parameters for optical images. The system can capture 15 sequential frames of flow images in one half second through the interface board.

The digital images are conveyed from a Macintosh II computer to Apollo computer workstation through NCSA Telet 2.2 software installed in Macintosh II. The data are in ASCII file format and ready to be used for quantitative velocity measurement by the digital vector velocimetry (DVV) method. Each image datum is a two-dimensional array of the dimension corresponding to the size of the interrogation window and every pixel has the integer value between 0 and 255 scaled by 8 bits. After the image data are loaded on the Apollo workstation, the DVV method is accomplished by executing the program written in M-scripes of MATLAB mathematical software. As a result of the DVV method the information of velocity vector is provided in ASCII file formats as output. Finally, velocity vector plots and velocity profiles can be obtained using MATLAB software.

3. Digital Vector Velocimetry Method

3.1 Digital vectorgram

In order to achieve the quantitative measurement of instantaneous velocity vector field with the DVV method one needs to construct a digital vectorgram in which all possible digital vectors are computed from the two sequential images and plotted from the same origin. A digital vector is defined as a vector formed between two time-sequential particle images. To construct a digital vector the image is first subdivided into many interrogating elements as shown in Fig. 3. In this study each typical element has 31×31 pixels. In the example shown three illuminated particles (i, k, m) in an element on the first image are assumed to translate to the pixel points (j, l, n) on the subsequent image. In the element there are numerous digital vectors that can be constructed from the flow images in the interrogating element as shown in Fig. 4. The plane that plots the number of possible vectors from the same origin is called the digital vectorgram as shown in Fig. 5. The most probable velocity vector is identified as the largest number, shown to be 3 in Fig. 5, of the digital vector on the vectorgram.

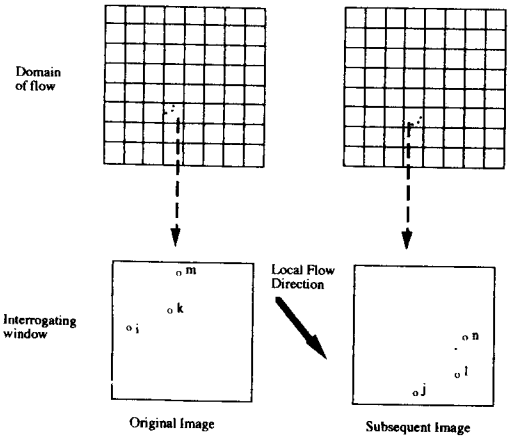

Fig. 3 Particle images in the interrogating window

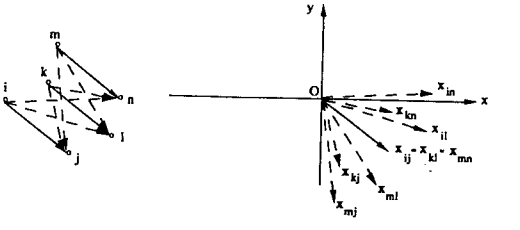

Fig. 4 Possible vectors from particle images

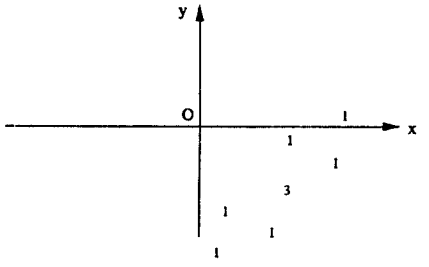

Fig. 5 Digital vectorgram (Assumption : $Q_i = Q_j = Q_k = Q_l = Q_m = Q_n = 1$)

In constructing the digital vectorgram, since both the time duration that separates images and the origins of these digital vectors are known, there will be no ambiguity in the velocity direction. As an example, let us consider the case of two time-sequential images. One may construct a set of digital vectors from the first image and the second. All these digital vectors have the definite magnitude and direction. Denote points (i, k, m) as the point in the original image and (j, l, n) in the subsequent image as shown in Fig. 3. From point k in the first image there are many possible image vectors that can be connected to any particle images on the second image (e. g., $k \rightarrow j$, $k \rightarrow l$, $k \rightarrow n$) as shown in Fig. 4. Similarly point i or m in the original image forms digital vectors ($i \rightarrow j$, $i \rightarrow l$, $i \rightarrow n$, $m \rightarrow j$, $m \rightarrow l$, $m \rightarrow n$). The vectors from k to l, from i to j and from m to n are respectively denoted as $\boldsymbol{x}_{kl}$, $\boldsymbol{x}_{ij}$, $\boldsymbol{x}_{mn}$ with the vector intensity Q_{kl}, Q_{ij}, Q_{mn}. The intensity of the digital vector $\boldsymbol{x}_{kl}$, Q_{KL}, is defined as the product of the digital intensity (gray level) at point k on the first image, Q_k, and that at point l on the second image, Q On the image detected by a CCD the level of digital intensity for Q_k or Q_l may vary from 0 to 255. On the digital vectorgram shown in Fig. 4 the digital vectors $\boldsymbol{x}_{kl}$, $\boldsymbol{x}_{ij}$ and $\boldsymbol{x}_{mn}$ are the same vectors but may have different intensities. In general, the resulting vector on the vectorgram has the sum of three intensities Q_{kl}, Q_{ij} and Q_{mn}. The resulting vector with the maximum digital intensity on the digital vectorgram may be considered to be the most preferred velocity vector for all particles in the interrogating element.

The digital vector field sampled within an interrogating window on the digital vectorgram is then given by

$$\mathrm{I}(\boldsymbol{x}) = \sum_{k=1}^{K} \sum_{l=1}^{L} Q_{kl}\ \delta[\boldsymbol{x} - \boldsymbol{x}_{kl}] \tag{1}$$

Here $\mathrm{I}(\boldsymbol{x})$ is the distribution of the intensities of the digital vectors on the digital vectorgram. K is the total number of the image particles in the original image, and L is the total number of the image particles in the subsequent image. K and L are not neccessarily equal. $\boldsymbol{x}_{kl} (= \boldsymbol{x}_l - \boldsymbol{x}_k)$ is the digital vector from k to l. $\delta[\cdot]$ is Dirac delta function. The digital vector that possesses the maximum intensity in $\mathrm{I}(\boldsymbol{x})$ is taken to be the representative velocity vector of the interrogating window. The window size in the present study is typically 31×31 pixels or equivalently to 9×9 mm^2 of the test section imaged. Figure 5 illustrates the distribution of $\mathrm{I}(\boldsymbol{x})$ from the two images shown in Fig. 3 with particle image intensity, Q_{kl}, set to be either 0 or 1.

It should be remarked that the DVV method is quite similar in concept to the statistical correlation method proposed by Willert and Gharib (1991). The difference is that the DVV method does the direct counting and uses discrete concept only.

3.2 Determination of velocity vector

Figure 6 illustrates graphically the DVV method when it is applied to two time-sequential image samples. In the figure, Dirac delta functions are used to represent particle images within 15×15 pixel interrogating window of two sequential images The digital vectorgram constructed for 15×15 pixel window will create a 29×29 pixel (x, y) domain to accomodate the positive or negative digital vector or $\mathrm{I}(\boldsymbol{x})$. The largest spike of $\mathrm{I}(\boldsymbol{x})$ displaced from the origin on the digital vectorgram (Fig. 6 c) corresponds to the most probable spatial shift of the particles in the interrogating region during the time between exposures. The smaller spikes are a result of digital vectors formed from particles pairing with other particles and not with themselves. These are essentially pseudovector or noise.

To achieve a stable and accurate prediction of

the most probable velocity vector when the particles in the interrogating window do not move uniformly, it is proposed that the digital vectorgram obtained in one interrogating window of 15 $\times$ 15 pixels is segmented into subregions, each of which has a size of 3×3 pixels and is overlapped two thirds of the area with the next. The digital vectorgram thus has 27×27 equally spaced subregions. The intensities of digital vectors in each subregion are integrated. When a subregion has the maximum integrated intensity, it is the indication of the most probable velocity vector. When the subregions are overlapped, the searching for the maximum-intensity subregion becomes easier compared with the case without overlapping. This procedure provides a stable and accurate determination of the velocity. In the summation of intensities, one may take the weighted average on the digital vectors by the intensity (i.e., centroiding technique) within the subregion. The vector corresponding to the resulting maximum intensity is then the representative velocity vector of the particles in the interrogating window. Employing the DVV method, the velocity vectors are thus determined. Once the representative displacement vector is obtained as $\boldsymbol{X}=(\triangle x)\boldsymbol{i}+(\triangle y)\boldsymbol{j}$, the magnitude and the direction of the velocity in the interrogating window are given by the followings :

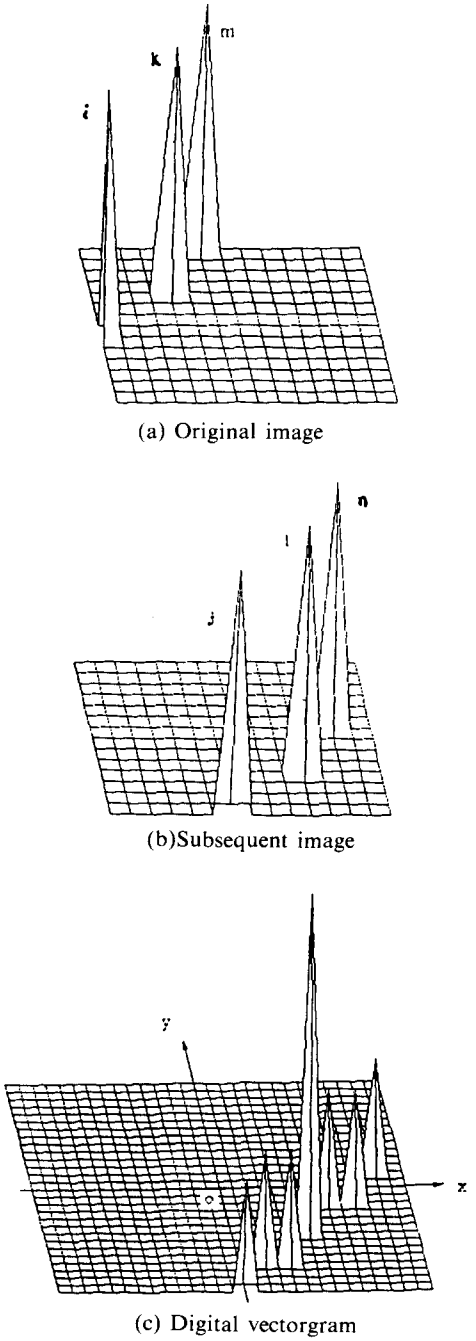

(a) Original image

(b)Subsequent image

(c) Digital vectorgram

Fig. 6 Three-dimensional view of digital vectorgram(c) obtained from image pair(a) and (b).

$$\theta=\tan^{-1}\frac{\triangle y}{\triangle x} \tag{2}$$

$$v=\frac{s}{MT} \tag{3}$$

where θ, an azimuthal angle from the x coordinate, is the phase of the velocity vector, v is the magnitude of the velocity vector, $s=[(\triangle x)^2+(\triangle y)^2]^{1/2}$, M is the conversion factor of the imaging system, and T is the time between exposures.

4. Data Correlation and Experimental Results

The representative velocity vector in an interrogating window, according to the DVV method, is determined by choosing the position of the most intense vector in a digital vectorgram. Because of digital characteristics, the accuracy of the velocity vector is limited to a pixel size. However, with a centroid method in the digital

vectorgram, a subpixel variation for velocity vectors is achieved. Also, many data can be generated by different pairings of two images at different time intervals. A criterion is established to verify the consistency of these data from different pairings of image data. A consistent result is obtained by requiring that data must be within the set values, typically with 5% of variation in magnitude and difference in direction of velocity vector at a certain point among data analyzed.

When a picture of the side view of a rotating flow is taken, the image plane is ditorted in the radial direction because of the curvature of the cylinder wall. Even though the actual flow is axisy mmetric, the side view image is not symmetric. This problem is resolved by taking the average of the two flow fields which cancels the difference created by the opposite rotation. Optical correction curve shown in Fig. 7 is also used to eliminate the optical distortion in the radial direction. The axisy mmetric flow field is thus achieved.

In the present study, the angular speed of the lid is set to 10 rpm with water as working fluid in a cylinder of 127 mm diameter and 127 mm height, which gives a Reynolds number of 3200 based on the diameter and the angular speed. The velocity vector plots from the digital vector velocimetry (DVV) method at this angular speed are compared with the qualitative pictures obtained using the particle streak velocimetry (PSV) method in Fig. 8, which is obtained by the

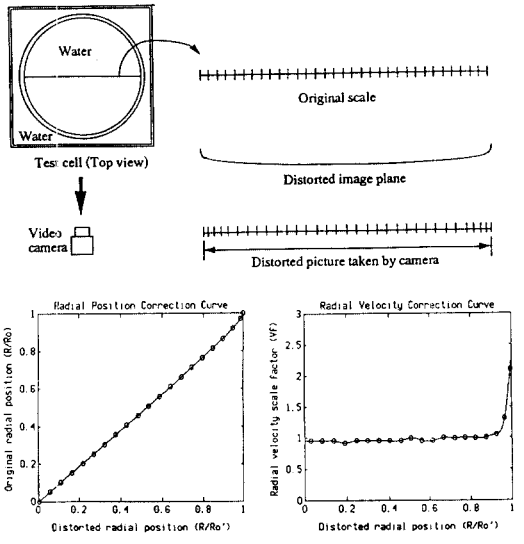

Fig. 7 Correction curves for lid-driven rotating flow with side wall (R_o ; original radius, R_o ; radius of distorted image)

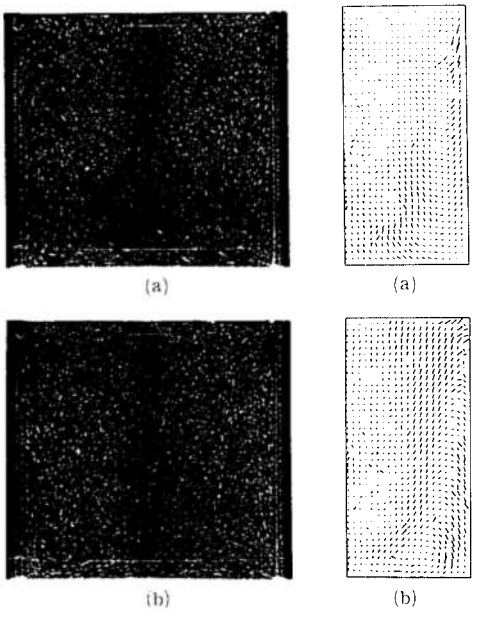

Fig. 8 Particle streak view and reslut of DVV measurement of lid-driven rotating flow with side wall($\omega=10$ rpm). (a) & (a)′ Counterclockwise rotation of lid, (b) & (b)′ Clockwise rotation of lid

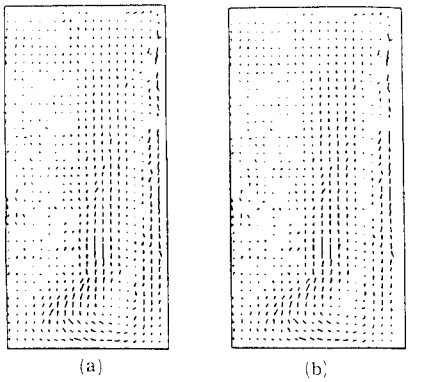

(a) Recovery of axisymmetric flow using average concept.
(b) Final distortion-corrected axisy mmetric flow field.

Fig. 9 Corrected side view flow field of lid-driven rotating flow with side wall($\omega=10$ rpm)

CCD camera with an exposure time of 0.8 s to create the particle streak image. It is seen that the two flow patterns with the opposite directions of lid rotation are not symmetrical and look different from each other. The actual flow pattern should be sy mmetrical according to the axisymmetry of the domain. For each case, the velocity vector pattern measured from the DVV method reveals good agreement with the particle streak view. Figure 9 shows the corrected side view through the optical corrections. Velocity vector plot (a) is a recovered axisy mmetric flow field by taking average of images (a)′ and (b)′ in Fig. 8. The final axisy mmetric flow field after taking correction of the rotational direction and correcting the radial distortion using the correction curves given in Fig. 7 is shown in plot (b) of Fig. 9.

5. Discussion

The finite analytic (FA) method is used to simulate the lid-driven rotating cavity flow and to compare the numerical results with the experimental data. The FA method was introduced and developed by Chen et al (1983 and 1984). Numerical and experimental results of the side view for Re=3200 are illustrated in Fig. 10. Numerical calculation for the lid-driven rotating cavity flow is conducted with staggered system of 42×22 grids, and results of velocity vector, streamfunction and pressure distribution are given in the figure. Further details of numerical analysis are given by Kim (1991).

As shown in pressure distribution, the maximum pressure is located just under the outer edge of the lid. This is created by the centrifugal force acquired by the viscous fluid from the rotation of the wall and then to return near the bottom against the radial direction toward the axis since the bottom wall is stationary. Because of axisymmetry of the test cell, the fluid converges toward the axis along the bottom. The fluid near the bottom is then merged into the upward moving region near the axis. The flow is then turned and accelerated upward along the axis until it reaches the minimum pressure region. Once the fluid

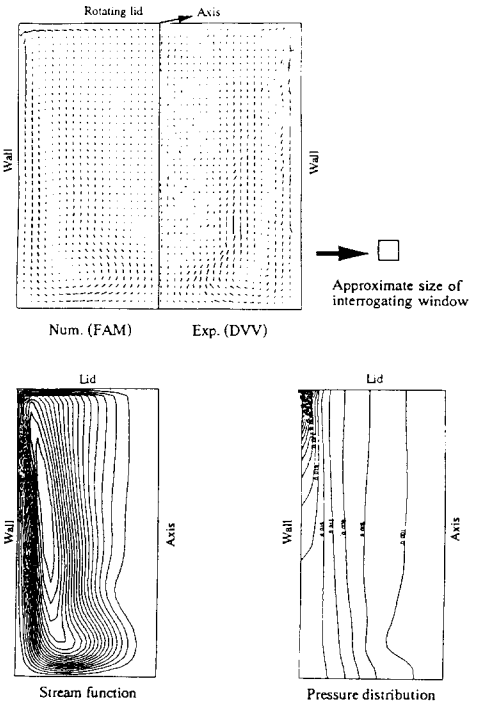

Fig. 10 Comparison of numerical results and experimental data of side view for lid-driven rotating cavity flow(Re=3200 or ω=10 rpm)

passes the minimum pressure zone it is decceleratd and at the same time deviated from the axis in the radial direction. Therefore the side view of the lid-driven rotating cavity flow shows that there exists a sharp turning region near the axis at the lower part of the test cell. Consequently the upper region near the axis is a region of relatively slow fluid motion. In summary, the general flow pattern in the X-R plane for the lid-driven rotating cavity flow includes a strong flow stream along the solid walls including the surface under the lid and the cylinder wall. Then the fluid in general diverges from near the axis towards the edge of the lid. The upper figure shows two quantitative velocity vector plots : one measured by the DVV method and the other predicted by the FA method.

In Fig. 11, numerical and experimental axial velocity profiles at four axial locations are compared. Generally the simulated results are in good agreement with the experimental data except the regions where the velocity vector changes

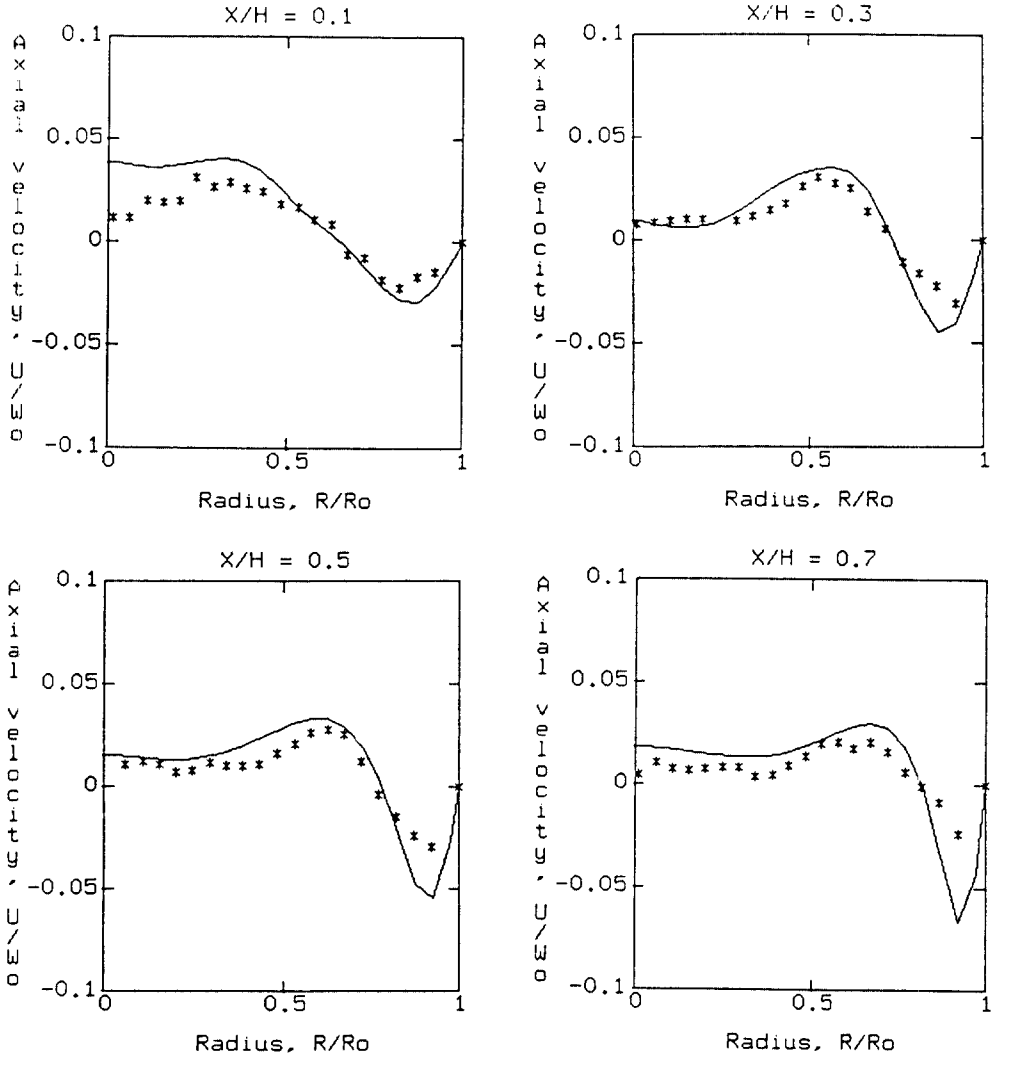

Fig. 11 Comparson of numerical and experimental axial velocity data for lid-driven rotating flow (Re=3200 or ω=10 rpm). solid line; FAM, *; Exp.(DVV).

rapidly or the gradient of the velocity profiles is so steep. In the regions, the magnitude of the velocity vector is considered to be underestimated by the smoothing effect, which is generated due to the considerable size of the interrogating window, about 9 mm 9 mm. This result can be improved using the finer CCD chip such as 1000×1000 pixels.

6. Conclusions

The DVV method counts directly the possible vectors between two sequential frames of images within an interrogating window and constructs the digital vectorgram that includes the intensity of each possible vector. The location of the maximum intensity on the digital vectorgram is then determined as the representative velocity vector in the interrogating window. The DVV method is shown to be logically simple and to save the computational time.

Laminar numerical results for the lid-driven rotating cavity flow are compared with the experimental data obtained by the DVV method. The

comparisons in the side view show good agreement except that there are some discrepancy in the steep velocity-gradient region near the wall or the axis of the lower domain.

The present experimental study by the DVV method may be improved to achieve higher accuracy in quantitative visualization. Higher power of the laser, higher acquisition speed system, and finer resolution of the CCD camera are needed to provide better accuracy of measurement and broader dynamic range of the velocity in the high Reynolds number flow including turbulent flow. Alternatively, a bigger test cell may be constructed for better accuracy. The finer image that covers only the partial domain can be taken and analyzed, and the velocity field for the whole domain can be obtained by combining the images of the partial domains.

Acknowledgement

This work is in part supported by Chonnam National University Research Funds.

References

Adrian, R. J., 1984, "Scattering Particle Charcteristics and their Effect on Pulsed Laser Measurements of Fluid Flow : Speckle Velocimetry vs Particle Velocimetry," *Applied Optics*, Vol. 23, pp. 1690~1691.

Adrian, R. J., 1991, "Particle-Imaging Techniques for Experimental Fluid Mechanics," *Annual Review of Fluid Mechanics*, Vol. 23, pp. 261~304.

Chen, C. J., Kim, Y. G. and Walter, J. A., 1993, "Progress in Quantitative Flow Visualization and Imaging Process," *Atlas of Visualization*, Vol. 1, pp. 279~296.

Chen, C. J. and Yoon, Y. H., 1983, "Finite Analytic Numerical Solution of Axisymmetric Navier-Stokes and Energy Equations," *Journal of Heat Transfer*, Vol. 105, No. 3, pp. 639~645.

Chen, C. J. and Chen, H. C., 1984, "Finite Analytic Numerical Method for Unsteady Two-Dimensional Navier-Stokes Equation," *Journal of Computational Physics*, Vol. 53, No. 2, pp. 209~226.

Hesselink, L., 1988, "Digital Image Processing in Flow Visualization," *Annual Review of Fluid Mechanics*, Vol. 20, pp. 421~485.

Kim, Y. G., 1991, "Development of Digital Vector Velocimetry Method and Its Application to Rotating Flows," Ph. D. Dissertation, The University of Iowa, Iowa City, Iowa.

Kim, Y. G. and Chen, C. J., 1992, "Development of Digital Vector Velocimetry Method and Its Application to Lid-Driven Rotating Flow," *Flow Visualization VI*, pp. 848~852.

Landreth, C. C., Adrian, R. J. and Yao, C.-S., 1988, "Double Pulsed Particle Image Velocimetry with Directional Resolution for Complex Flows," *Experiments in Fluids*, Vol. 6, pp. 119~128.

Merzkirch, W., 1987, *Flow Visualization*, 2nd Edition, Academic Press, New York.

Walter, J. A. and Chen, C. J., 1989, "Flow Visualization of Particle Streaks in Offset Channel Flow by a Direct CCD Imaging Process," *The Winter Annual Meeting of ASME*, San Francisco, CA, FED-Vol. 85, pp. 115~120.

Willert, C. E. and Gharib M., 1991, "Digital Particle Image Velocimetry," *Experiments in Fluids*, No. 10, pp. 181~193.

Yang, W. J., 1988, *Handbook of Flow Visualization*, Hemisphere Publishing Company.